Mem. S.A.It. Vol. 83, 352

Memorie della

Strong gravity studies with the Large Observatory For X-ray Timing (LOFT)

E. Del Monte[1] and I. Donnarumma[1] on behalf of the LOFT consortium[2]

[1] INAF IASF Roma, Via Fosso del Cavaliere 100, I-00133 Roma, Italy
e-mail: [ettore.delmonte;immacolata.donnarumma]@iasf-roma.inaf.it
[2] http://www.isdc.unige.ch/loft/index.php/loft-team/consortium-members

Abstract. High-time-resolution X-ray observations of compact objects provide direct access to strong-field gravity, to the equation of state of ultradense matter and to black hole (BH) masses and spins. A 10 m^2-class instrument in combination with good spectral resolution is required to exploit the relevant diagnostics and answer two of the fundamental questions of the European Space Agency (ESA) Cosmic Vision Theme "Matter under extreme conditions", namely: does matter orbiting close to the event horizon follow the predictions of general relativity? What is the equation of state of matter in neutron stars? The Large Observatory For X-ray Timing (LOFT), selected by ESA as one of the four Cosmic Vision M3 candidate missions to undergo an assessment phase, will revolutionise the study of collapsed objects in our galaxy and of the brightest supermassive black holes in active galactic nuclei. Thanks to an innovative design and the development of large-area monolithic silicon drift detectors, the Large Area Detector (LAD) on board LOFT will achieve an effective area of ~12 m^2 (more than an order of magnitude larger than any spaceborne predecessor) in the 2–30 keV range (up to 50 keV in expanded mode), yet still fits a conventional platform and small/medium-class launcher. With this large area and a spectral resolution of <260 eV, LOFT will yield unprecedented information on strongly curved spacetimes and matter under extreme conditions of pressure and magnetic field strength.

Key words. Space vehicles: instruments – Black hole physics – Equation of state – Dense matter – X-rays: binaries – Stars: neutron

1. Introduction

1.1. The properties of ultradense matter

One of the key goals of high-energy astrophysics is to determine the equation of state (EOS) of ultradense matter, i.e. the relation between density and pressure at the highest possible densities, where the physics of quarks and quantum chromodynamics (QCD) come into play.

The high-density/low-temperature region of the QCD phase diagram is inaccessible to terrestrial laboratories and can only be probed astrophysically, where the ultradense matter EOS manifests as a mass-radius (M-R) rela-

Send offprint requests to: E. Del Monte & I. Donnarumma

tion for neutron stars (NS), whose cores contain the densest matter known. Model EOSs may be classified in two classes defined by the maximum neutron star mass that the EOS can sustain: the "soft" ones have a maximum mass in the 1.5–1.7 solar masses ($M_\odot$) range while the "stiff" ones can reach up to 2.4–2.5 $M_\odot$ (Lattimer & Prakash 2001). Recently, a heavy neutron star of 1.97±0.04 $M_\odot$ has been measured through accurate timing of a millisecond radio pulsar in a relativistic binary (Demorest et al. 2010), ruling out most soft EOSs and limiting the presence of quark matter in the neutron star core.

This is an important step, but the quest for the neutron star EOS is far than settled. We still do not know the typical radius or the maximum mass that a star can support before collapsing into a black hole.

Neutron star masses are measured with great precision from binary radio pulsar timing. However, neutron star radius measurements are particularly challenging, and no reliably precise measurements are available so far. Even more challenging is the difficulty to obtain simultaneous measurement of both M and R, which would allow clear discrimination between EOS models. The best tool to constrain the neutron star EOS is the modelling of coherent X-ray pulsations, that are detected in accretion-powered millisecond X-ray pulsars and during thermonuclear explosions on the surface of many accreting neutron stars ("type I" bursts).

The amplitude of pulsations caused by the emission from rotating "hot spots" on the surface is shaped by gravitational self-lensing by the neutron star's strong gravity which strongly depends on the neutron star M/R ratio. Similarly, the shape of the pulse is affected by the stellar rotational velocity (which depends on the star's radius and hot spot latitude) and by the binary inclination.

Modeling the variations of the pulse shape in different energy bands and at different luminosity levels has been demonstrated effective in constraining mass and radius (Leahy et al. 2009). Simulations based on RXTE results show that LOFT can achieve ~5% precision in radius measurement with such observations. Effective discrimination between different families of EOSs will be possible only with such a relative precision.

1.2. Strong gravity and the mass and spin of black holes

Most of the power generated by accretion onto neutron stars and black holes is released deep in the gravitational potential wells of these objects. Observation of the motion of matter in the innermost regions of accretion disks contains unique information on the properties of the strongly curved spacetime near neutron stars and black holes, and on the compact object's mass, spin and size.

Over the last two decades powerful diagnostics of the innermost disk regions have been discovered: among those based on timing measurements are the QPOs in the flux of a number of X-ray binary systems (and until now one active galactic nucleus) which occur at the dynamical time scale of the innermost disk regions and hence are associated to the fundamental frequencies of matter motion in strong field gravity. The Fe K_α emission lines which are observed in many accreting collapsed objects, from neutron stars to supermassive black holes in AGNs, are powerful spectral diagnostics that form a second, independent probe of the same strong field gravity regions.

The exploitation of these diagnostics has so far been hampered by insufficient throughput and/or energy range and resolution of the instrumentation. For instance, in about 20 neutron star binary systems, a diverse QPO phenomenology was observed with RXTE. At high frequencies (200–1200 Hz), pairs of signals are observed, whose frequencies vary on timescales as short as hundreds of seconds.

These signals can be strong, but their intensity is highly variable. Averaging these signals over thousands of seconds, sometimes days in order to detect them, has until now prevented the exploitation of the full potential of this diagnostic.

A somewhat similar phenomenology is observed in several black holes, but their QPOs are weaker and even more difficult to detect, especially at high frequencies.

1.2.1. Neutron star and stellar mass black hole

The major leap in the effective area that LOFT provides will permit for the first time to exploit new techniques for extracting physical information from the QPOs. In the following we describe a few examples of this. Methods have been devised to test theoretical models through detailed high signal to noise observations. For instance, in the parametric epicyclic resonance model two of the oscillation modes are associated with a resonance of the relativistic radial and vertical epicyclic frequencies (Abramowicz & Kluźniak 2001); in the relativistic precession model instead, the highest frequency signal is identified with the azimuthal frequency of motion, while two of the modes arise from relativistic nodal and periastron precession (whose frequency are related also on the epicyclic frequencies (Stella et al. 1999). By studying the QPO behavior as a function of source intensities LOFT will afford to remove the current degeneracy in the interpretation of the oscillation. Fig. 1 shows simulated LOFT results in the two models for a transient black hole. The two predictions are very different and hence LOFT/LAD easily discriminates between the two models where with current instruments both remain viable. Once the ambiguity in the interpretation of the QPO phenomena is resolved, the frequencies of the QPO themselves, which LOFT measures with high precision, will immediately provide access to yet unobserved general relativistic effects (Lense-Thirring and strong field periastron precession) and allow us to derive or tightly constrain the black hole mass and spin. LOFT will enable the study of the QPO signals in time (as opposed to Fourier) domain; in particular, low frequency QPOs will be studied in individual pulses and kHz QPO within their coherence timescale. The latter requires a minimum effective area of $\sim$10 m^2.

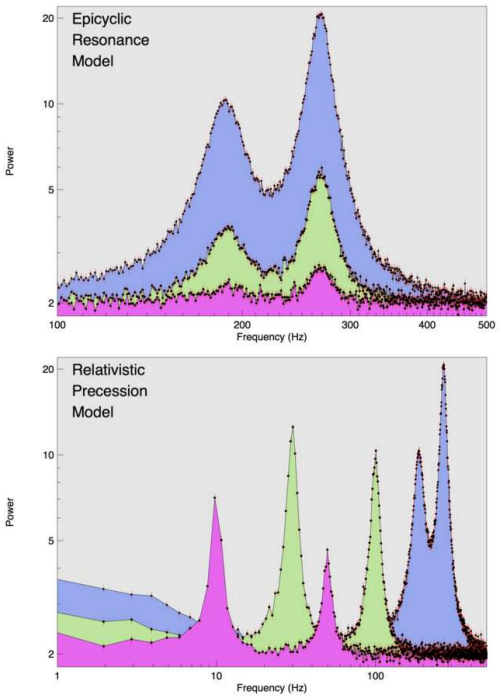

Fig. 1. LOFT simulated time evolution of power spectra for the Epicyclic Resonance Model (top panel) and the Relativistic Precession Model (bottom panel). Adapted from Feroci et al. (2011).

1.2.2. Supermassive black holes

Bright AGN provide a complementary opportunity to study strong field gravity. Though their flux at the Earth is typically 100–1000 times lower than that of accreting black holes in galactic binaries, their dynamical timescales (which scale with the mass) are $\sim 10^6$ times longer. The result is that some 10^3 times more photons are received at the Earth per dynamical timescale from bright AGNs than from X-ray binaries. Therefore bright AGN provide a parallel channel for investigating very short term phenomena, such as the motion of a single spot in the disk or the response of the Fe-line disk emissivity to flares from the illuminating source. As in X-ray binaries, the relativistic broad Fe-line profile that is seen in the X-ray spectrum of a number of AGNs (about 70% of bright Seyfert 1), provides a powerful tool to investigate the accretion flow in a region where the motion is determined by General Relativity (Fabian et al. 1989; Laor 1991). LOFT will determine with very high signal to noise and accurate continuum subtraction the profile of

AGN Fe K-lines, thanks to its sensitivity and broad energy range. The instrumental and cosmic background in the LAD will permit to study AGNs in this context down to flux level of ∼1 mCrab. By assuming e.g. a 3 mCrab flux, with an exposure of 10^3 s LOFT will collect more than 5×10^5 counts in 2–30 keV, that will provide a high enough S/N to detect broad Fe lines, allowing us to measure the inner radius of the disk down to the marginally stable orbit and, from this, derive the spin of the BH. Moreover, LOFT's very high throughput will permit to investigate the line response to the orbital motion of individual blobs illuminated by the central source through the moving features that they induce in the line profile (Dovčiak et al. 2004). These "reverberations" will provide the physical unit for the emitting radius that is required to measure also the black hole mass in addition to the spin. An example of the expected performance of LOFT on this subject are shown in Fig. 2.

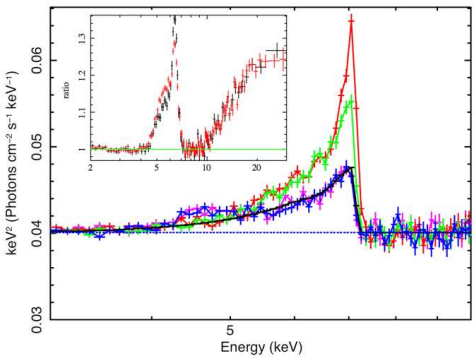

Fig. 2. Simulated LOFT/LAD spectra of a 3 mCrab (2–10 keV) AGN. The relativistic Fe line is produced in the innermost region of the accretion disc, extending down to the marginally stable orbit of a BH (spin a=0.99, mass of 3.6×10^6 $M_\odot$ and inclination of 45°). The variable Fe K feature is produced by an orbiting spot at $r = 10\ GM/c^2$ on the disk surface, illuminated by a flare. The orbital period is 4 ks and the total exposure is 16 ks. LOFT/LAD will track the line variation on 1 ks time scale, thus allowing a determination of the orbital period through measurements at four different orbital phases over four cycles. The inset shows two 10 ks spectra from simulated high (6 mCrab in 2–10 keV) and low (2 mCrab) flux states LOFT/LAD observations of MCG-6-30-15. Adapted from Feroci et al. (2011).

1.3. Observatory science

Besides the main science goals outlined above, LOFT will very successfully exploit the physical information contained in the flux variability of many different classes of sources. For this purpose the payload is equipped with a coded aperture Wide Field Monitor (WFM), described in Sect. 2.2 . The longer timescale variability will be explored by the WFM, singling out specific source activities and/or spectral states (e.g. those of accreting millisecond transient pulsars) amongst many hundreds of monitored sources. Clearly the WFM will be essential to trigger and carry the LAD observations required to achieve LOFT's main science objectives. In the following we briefly outline some of additional science themes to which LOFT will give great contributions.

X-ray binaries are the brightest sources of the X-ray sky. LOFT will be able to detect periodicities of unprecedented small amplitude and measure their phase and period evolution to high accuracy.

Millisecond radio pulsars also emit in the X-ray band. A large number of γ-ray sources have been discovered with Fermi, that are suspected to be fast rotation powered pulsars. A large area hard X-ray timing mission like LOFT should be able to detect the pulsations from many such objects.

The mechanism for the launching of jets is still poorly understood. The WFM's excellent sensitivity will allow us to trigger early on new X-ray transients, and hence to use the LAD for multi-wavelength campaigns with optical and IR instruments with sub-second time resolution, allowing for the estimate of the jet speeds over a wide range of luminosities for the same sources. It will lead to determine relations between jet speeds and luminosities and accretion states.

The WFM large instantaneous field of view is another important advantage of LOFT over past soft X-ray all-sky instruments. This gives LOFT an unprecedented capability for detecting rare, short-lived, bright sources, such as Gamma Ray Bursts, X-ray flashes, X-ray transients of all classes , and for obtaining high cadence monitoring of moderately bright sources.

2. Instrumentation

To meet the scientific requirements summarized in Table 1 and to achieve the science objectives summarized in Sect. 1, the LOFT scientific payload is composed of two instruments: the Large Area Detector (LAD) and the Wide Field Monitor (WFM). Both instruments are based on the technology of the large-area Silicon Drift Detectors (SDDs), although with application-specific detector design details. The LAD is composed of six Detector Panels (DPs) deploying from an optical bench and hosting at its center the WFM, a coded aperture instrument that observes a wide sky region, including the field of view of the LAD. A sketch of the LOFT structure is shown in Fig. 3.

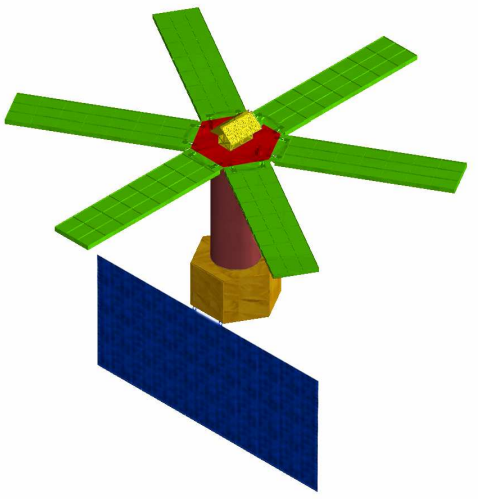

Fig. 3. Conceptual scheme of the LOFT satellite. (green) Large Area Detector, (yellow) Wide Field Monitor, (red) Optical Bench, (purple) Structural Tower, (gold) Bus and (blue) Solar Array. Adapted from Feroci et al. (2011).

2.1. The Large Area Detector (LAD)

The LAD is a collimated experiment, conceptually similar to its predecessors (e.g. RXTE/PCA, Jahoda et al. 2006). The development of a 10 m^2-class experiment is now made possible by the recent advancements in the field of large-area Silicon Drift Detectors (SDDs) and micro capillary-plate (MCP) X-ray collimators. The relevant feature of the LOFT design is the low mass and power per unit area enabled by these two elements. A comparison of the effective area of LOFT and other past and future instruments for X-ray timing (e. g. RXTE-PCA, XMM-EPIC-pn, ASTROSAT-LAXPC and IXO-HTRS) is shown in Fig. 4.

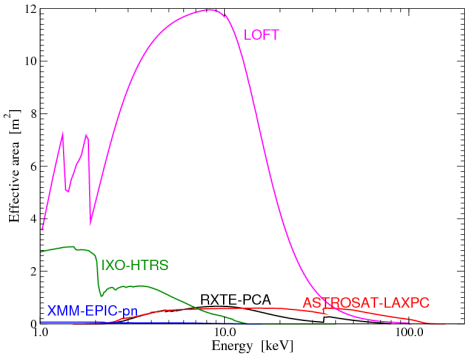

Fig. 4. LAD effective area plotted in linear scale vs. energy, as compared to that of other satellites for X-ray astronomy. Adapted from Feroci et al. (2011).

2.1.1. Silicon Drift Detector (SDDs)

The SDDs are based on the heritage of the detectors (Rashevsky et al. 2002; Vacchi et al. 1991), developed by INFN Trieste (Italy) in co-operation with Canberra Inc., for the Inner Tracking System in the ALICE experiment of the CERN Large Hadron Collider.

Table 1. Scientific requirements for the LOFT LAD and WFM instruments.

LAD		
Parameter	Requirement	Goal
E range	2–30 keV (nominal) 2–50 keV (expanded)	1–40 keV (nominal) 1–60 keV (expanded)
Eff. area	12.0 m^2 (2–10 keV) 1.3 m^2 (@30 keV)	15 m^2 (2–10 keV) 2.5 m^2 (@30 keV)
ΔE (FWHM, @6 keV)	<260 eV	<180 eV
FoV (FWHM)	<60 arcmin	<30 arcmin
Time res.	10 μs	5 μs
Dead time	<0.5% (@1 Crab)	< 0.1% (@1 Crab)
Background flux	<10 mCrab	< 5 mCrab
Max. src flux (steady)	>0.3 Crab	>10 Crab
Max. src flux (peak)	>15 Crab	>30 Crab
WFM		
Parameter	Requirement	Goal
E range	2–50 keV	1–50 keV
ΔE (FWHM)	<300 eV	<200 eV
FoV (FWHM)	>3 steradian	>4 steradian
Ang. res.	5 arcmin	3 arcmin
PSLA	1 arcmin	0.5 arcmin
Sens. (5σ, 50 ks)	2 mCrab	1 mCrab
Sens. (5σ, 1 s)	0.5 Crab	0.2 Crab

The LAD detector design is indeed an optimization of the ALICE detector: 6-inch, 450 μm thick wafers will be used to produce 76 cm^2 monolithic SDDs (108.52 mm × 70.00 mm active area). The anode pitch is increased to 854 μm (corresponding to an elemental area of 0.854 mm × 35 mm = 0.299 cm^2) to reduce the power consumption and improve the low-energy response. The Si tile is electrically divided in two halves, with 2 series of 128 readout anodes at two edges and the highest voltage along its symmetry axis. The drift length is 35 mm. A drift field of 370 V/cm (1300 V maximum voltage), gives a maximum drift time of $\sim$ 5 μs (Kushpil et al. 2006), constituting the detector contribution to the uncertainty in the determination of the time of arrival of the photon. Indeed, with the above electric field, the charge will typically distribute over one (40 % of events) or two (59 % of events) anodes, rarely on three (1 % of counts). The segmentation of the detector makes the dead time and pile-up risks negligible (see below), a crucial property for a timing experiment. The detectors are able to time tag an X-ray photon with an accuracy < 10 μs and an energy resolution of <250 eV FWHM.

We measured an energy resolution of <300 eV FWHM on single anode events with the low energy discrimination threshold below 0.6 keV (see Zampa et al. 2011, for details) from an ^{55}Fe source (with lines at 5.9 and 6.5 keV)

in our laboratory at IASF Roma at a temperature of $\sim$ 20° C, by instrumenting a spare ALICE SDD with discrete electronics. The detectors as optimized for the LOFT application will achieve even better performance by the use of an integrated read-out electronics, that will largely reduce the parasitic capacitance, and by the instrument operation at low temperature, decreasing the leakage current by more than an order of magnitude, even in the larger thickness and pitch configuration of LOFT, as well as with the expected level of radiation damage in orbit.

2.1.2. Micro capillary plates collimators

The other key element of the LOFT payload innovative design is the capillary plate X-ray collimator, based on the technology of microchannel plates (although collimators based on the same technology were already used in the Medium Energy experiment aboard EXOSAT, Taylor et al. 1981). The LOFT baseline is a multi-pore sheet of lead glass, with 2 mm thickness, inner hole diameter of 25 μm and pitch of 28 μm (resulting in a field of view of 43 arcmin FWHM and open area ratio of 80 %), able to absorb soft X-rays coming from outside its aperture holes. Standard collimators can be procured off-the-shelf with a 50 % lead content in the glass, offering a significant stopping power to soft X-rays at a weight of only $\sim$ 3 kg m^2, enabling large areas at reasonable mass and costs. We studied the angular response to different photon energies with GEANT Monte Carlo simulations and the results demonstrate an effective shielding up to $\sim$ 40 keV, above the energy range of LOFT. Photons with higher energy passing through will be detected with low efficiency by the thin Si detector and will be anyway discriminated by their energy deposition, except for the Compton interactions that will contribute to the residual instrumental background.

2.2. The Wide Field Monitor (WFM)

The WFM is a coded aperture instrument, composed of four cameras for a total geometric area of 1600 cm^2, hosted on the top of the LAD tower. The coded mask imaging is the most effective technique to observe simultaneously steradian-wide sky regions with arc min angular resolution. The WFM is designed on the heritage of the SuperAGILE experiment, successfully operating in orbit since 2007 (Feroci et al. 2007, 2010, see e. g.), that demonstrated the feasibility of a compact, large-area, light and low-power, arc minute resolution X-ray imager, with steradian-wide field of view. The LOFT/WFM applies the same concept, with improvements provided by the superior performance of the large area SDDs, allowing to reach an energy resolution < 300 eV and to reduce the energy threshold down to 2 keV.

In contrast to their use in the LAD, in the WFM the position resolution of the SDD is a key issue. For this reason the baseline WFM SDDs have the default $\sim$ 300 μm anode pitch (similar to the ALICE SDDs). Using the lab tests of the ALICE spare detector and an accurate Monte Carlo simulation of the detector physics, exploiting the electron cloud diffusion during the drift, we estimated a position resolution better than 60 μm along the anodes and $\sim$ 5 mm along the drift channel (Campana et al. 2011). Due to the coarse detector position resolution along the drift direction, we conservatively consider the WFM camera as 1-D and we require two orthogonal cameras to image the same sky region at any time for fine source positioning in 2-D, similar to SuperAGILE, RossiXTE/ASM and HETE-2/WFM.

The design of a single WFM camera (see Fig. 5) consists of a tiled 20 cm $\times$ 20 cm detector plane (6 large-area 450 μm thick SDDs), an asymmetric 2-D coded mask and a collimator. With a detector position resolution < 100 μm, a 150 μm thick Tungsten mask with a pitch of $\sim$ 200 μm and ~10 mm in the two directions, at a ~150 mm distance provides an angular resolution <5 arc min. The SDD readout employs the same ASICs as the LAD, with a proper design customization to the finer pitch. A light collimator (e.g., 1 mm thick carbon fibre, covered with a 150 μm Tungsten sheet) effectively shields the X-ray photons from the diffuse X-ray background (the main background source, as charged particles are efficiently rejected by

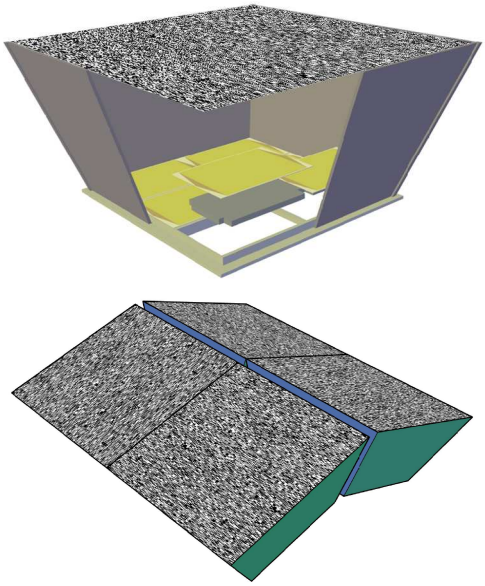

Fig. 5. The Wide Field Monitor. Top: design of a single camera. Bottom: the four camera units. Adapted from Feroci et al. (2011).

the amplitude discrimination) up to energies above 60 keV. The overall WFM design includes four identical camera units assembled in a configuration where an orthogonal set of 2 cameras monitors the same sky region. The two sets are oriented at 37° to each other. The WFM total volume is $4 \times (30 \times 30 \times 15\ \mathrm{cm}^3)$, while the total mass, including 20 % margin, is estimated as 37.0 kg. The WFM total power consumption is estimated, including margin, as 12 W. As a baseline, due to telemetry limitations, the WFM will not operate in photon-by-photon mode at all times. Images in different energy ranges every 300 s, 0.1 keV resolution energy spectra every 30 s and light curves (with bin size of 16 ms) will be onboard integrated and pre-processed by the BEEs and PDHU, similarly to what is routinely done by Swift/BAT. A triggering algorithm will scan time series and images to detect fast transients, e. g., X-ray bursts or Gamma Ray Bursts. Upon trigger, ∼ 300 s of photon by photon data will be downloaded to the telemetry.

3. Discussion

CHRISTIAN MOTCH: On how many AGNs will LOFT be able to do reverberation mapping?
IMMACOLATA DONNARUMMA: On the basis of the study led by de La Calle Pérez et al. (2010), we expect to study the reverberation mapping on about ten AGNs.

References

Abramowicz, M.A. & Kluźniak, W., 2001, A&A, 374, L19
Campana, R. et al., 2011, NIM A 633, 22
de La Calle Pérez, I., et al., 2010, A&A, 524, id.A50
Demorest, P.B. et al., 2010, Nature 467, 1081
Dovčiak, M. et al., 2004, MNRAS 350, 745
Fabian, A.C., et al. 1989, MNRAS, 238, 729
Feroci, M. et al. 2011, arXiv:1107.0436, Exp. Astr., in press
Feroci, M. et al. 2010, A&A 510, A9
Feroci, M. et al. 2007, NIM A 581, 728
Jahoda, K., et al., 2006, ApJSS, 163, 401
Kushpil, S. et al. 2006, NIM A 566, 94
Laor, A., 1991, ApJ, 376, 90
Lattimer, J.M., Prakash, M., 2001, ApJ, 550, 426
Leahy, D.A., et al. 2009, ApJ, 691, 1235
Rashevsky, A. et al. 2002, NIM A 485, 5460
Stella, L., et al., 1999, ApJ 524, L63
Taylor, B.G. et al. 1981, Space Sci. Rev. 30, 479. DOI 10.1007/BF01246069
Vacchi, A. et al. 1991, NIM A 306, 187
Zampa, G. et al. 2011, NIM A 633, 15